

23rd International Conference on Material Forming (ESAFORM 2020)

On the Mechanism of Formation of Back-End Defects in the Extrusion Process

Henry Sigvart Valberg^{a*}, Martin Lefstad^b, André Luiz de Moraes Costa^c

^aProf. Valberg Consulting, Planetv. 15b, 7036 Trondheim, Norway

^bSINTEF Industry, Postboks 4760, Torgarden, 7465 Trondheim, Norway

^cDepartment of Mechanical Engineering, Federal University of Sergipe, Brazil

* Corresponding author. Tel.: +47-7491897604; E-mail address: valberg.henry@gmail.com

Abstract

FEM-analysis is applied to study metal flow in aluminum extrusion with focus on how material flow defects form when the last part of the billet is extruded through an axisymmetric die. First, an overview is given of the current state of art of knowledge regarding formation of typical rear-end defects in metal extrusion. Afterwards the software DEFORM is used to model the extrusion process. It is shown how this software describes the inflow of inferior material from the outer surface and subsurface of the billet, into the core of the rear-end of the billet during the extrusion stroke. Special attention is paid on trying to understand the mechanism of formation of common defects like the funnel defect and the coring defect in the extrusion process.

© 2020 The Authors. Published by Elsevier Ltd.

This is an open access article under the CC BY-NC-ND license (<https://creativecommons.org/licenses/by-nc-nd/4.0/>)

Peer-review under responsibility of the scientific committee of the 23rd International Conference on Material Forming.

Keywords: Extrusion defects; formation mechanisms of defects

1. Introduction

In aluminum extrusion, a general problem is that defects tend to form in the interior of the extruded rod in the last part of the extrusion stroke. In technical literature, it is therefore common to name such defects as back-end defects. Two different defects form this way in the last part of the extrusion press cycle; they are commonly named as coring or funnel formation. The difference between these two defects is perhaps best explained by showing FEM-simulation pictures of the rear-end part of the extrudate and the extrusion discard, as they appear before the discard is partitioned from the extruded rod, see Fig. 1. The funnel defect is shown at top of the figure as the hollow void (or funnel) formed in the center of the rod. Another common name for this defect is piping.

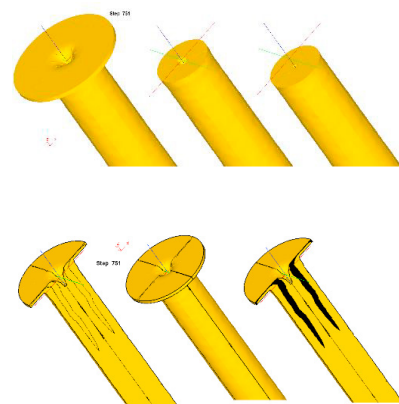


Fig. 1. Funnel formation (top view) and coring in extrusion (bottom view).

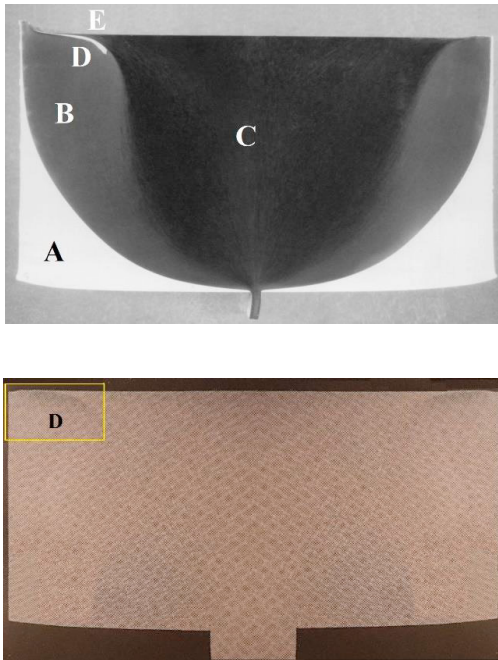


Fig. 2. Coring as observed by means of metallography [1].

The term piping is used because the rear-end of the obtained extrusion appears as a pipe when the defect is present. The presence of the funnel defect can to a large degree be avoided if extrusion is performed with high friction between the ram and the back-end surface of the billet.

Coring is another defect formed in the back-end of the rod. This defect is caused by inflow of contaminated metal from the outer surface of the billet towards the core of the billet during the extrusion cycle. In the late stages of extrusion, this contamination finally flows through the die and creates a defect near to the core in the back-end portion of the extruded rod.

In Fig. 1 (bottom view) is shown how the material layer (region inside yellow rectangle with darker color), which in the beginning of the stroke made up the outer surface layer of the billet, has flowed backwards and inwards into the rear-end of the billet. Later during extrusion this material will flow further from here forward in the extrusion direction, to appear in the rod in a location half-way between the rods surface and center. If enough contamination follows along with the billet surface during this movement, the material in the core may split apart from the material in the outer part of the rod. To summarize, one can say that the funnel defect is present in the center of the rod; the coring defect in a location between the center and the surface of the rod. If a cross-section is cut through the back-end of the rod both defects may be visible in the same section of the extrudate.

Recording of metal flow in extrusion processes is often done by use of scratched grid patterns on two longitudinally sectioned billet halves added together before extrusion. Other methods are use of metallography or inserts of contrast materials in the billet. Fig. 2 shows how the phenomenon of coring is observed by metallography. A partially extruded

billet is removed from the container and sectioned longitudinally. The sectioned surface is machine and then ground on emery paper, finally etched using an appropriate etchant. After the treatment, the appearance of the sectioned surface will depend on the deformations subjected to the material of the billet. The photo at top of Fig. 2 reveals, as an example, the result when firstly a billet of alloy AlMgSi has been extruded to leave a disc of this billet material, of thickness approximately equal to the billet radius in the container, then secondly extruding a billet of AlMgZn on top of the remaining material in the container.

Different regions of flow revealed in this figure is the dead zone (A), sheared material (B) produced by the shearing action between the billet core and the surface layer of the billet (which sticks to the container wall during extrusion), the center portion of the billet (C) which is about to flow through the primary deformation zone ahead of the die. Finally, there is billet subsurface metal that flows into the interior of the billet (D) at the rear-end corner of the billet, later to appear as the coring defect. Because different alloys with different etching properties were applied in the experiment, one alloy can be distinguished from the other because the two alloys develop different colors upon etching. While AlMgSi appears with light Al-color the other alloy becomes black. In addition, in this experiment, a slice of AlMgSi-alloy (E) was scraped-off from the container wall by the advancing ram head during the extrusion stroke, and the slice flowed along the path of the movement of the coring defect.

Moreover, in the photo at bottom of Fig. 2, is shown how the flow of contaminated material (D) from the billet surface appears in a long billet discard, when only one single alloy is extruded. The contaminated material (marked by yellow rectangle) in the rear-end of the billet is visible in the etched longitudinal section of the partially extruded billet because it has darker color than the rest of material in the discard.

To mention is extensive experimental work done by Lefstad and Reiso [2], to map the flow behavior of the peripheral surface layer of billets in aluminum extrusion. They added thin inserts of contrast material into the billet surface, with flow stress of inserts approximately balanced to equalize the flow stress of the billets base metal. Results obtained in their experiments, in terms of longitudinal sections cut through such partially extruded billets, are shown in Fig. 3.

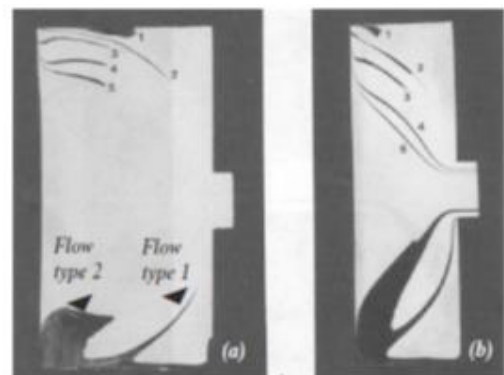


Fig. 3. Flow paths of the subsurface layer of the billet [2].

As shown at the bottom side of the extrusion discards in Fig. 3 a subsurface layer of given thickness does not flow evenly forward over the whole length of the billet. Instead there is exaggerated flow in two locations along the billet length. Firstly, near to the die hole the layer of marker material tends to flow inwards on top of the dead zone present in the corner between die and container. Secondly, at the rear-end corner between the billet and the container wall, the marker material accumulates, and thickens, concurrently as it flows inwards towards the core of the billet, and from here down towards the die exit. In [2] the two different kinds of exaggerated flow were denoted as flow type 1 and 2, respectively.

As regards the formation of the funnel defect in extrusion the mechanism by which this defect is formed is rather simple to describe. When the remaining amount of billet material in the container becomes small towards the end of the stroke, i.e., when there is only a thin disc of remaining billet material in between the die and the ram head, the surface of the billet in contact with the ram head becomes sucked-in into the extrusion material, so that a void forms in the center of the back-end of the billet. Upon further extrusion, this void grows and flows through the die hole, where it appears in the center of the extruded rod as a hole. A typical funnel defect formed in aluminum extrusion, at the stage shortly before it flows into the rod, is shown in Fig. 4.

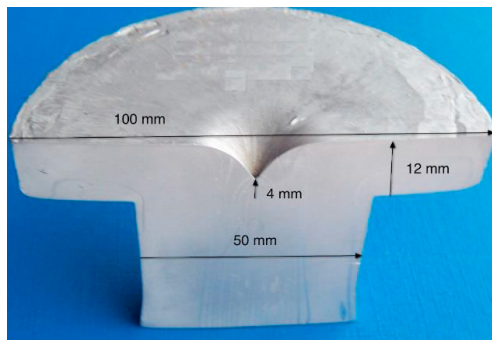


Fig. 4. Funnel formation in rod extrusion.

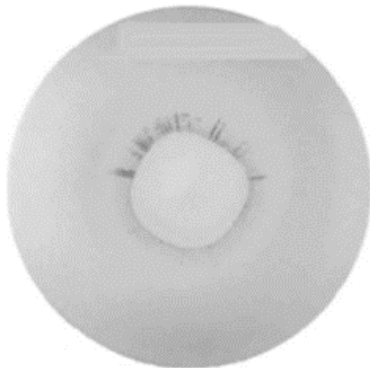


Fig. 5. Coring defect in cross-section cut through the back-end of an extruded rod [3].

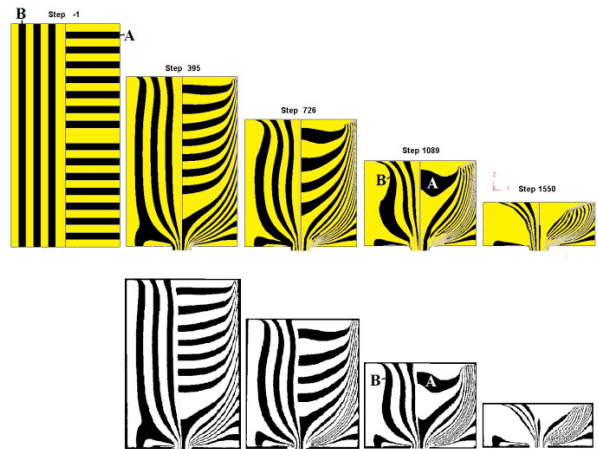


Fig. 6. Metal flow in laboratory extrusion judged from grid pattern (at top) and the same pattern obtained in FEA (at bottom).

However, as regards formation of the coring defect, the deformation mechanism that causes this defect, is more complex and has not yet been fully explained in the literature. The general explanation is that the defect is generated as a result of the inflow into the core of the rear-end of the billet of the contaminated outer surface layer of the billet, i.e. by flow type 2 shown in Fig. 3. Therefore, in this article we will use FEM-analysis supported by experimental information to compute metal flow in aluminum extrusion. Aim of the work is to bring forward a better understanding of the mechanism by which the coring defect forms in the extrusion process.

How this defect appears in the rear-end of a cross-sectioned metallographic section cut through the extruded rod is shown in Fig. 5. In an etched section cut from the rod the material in the core appears with brighter color than the slightly darker outer sleeve of the rod, and with contaminated material as a dark black (or grey) ring of material between the core and sleeve of the rod.

2. FEA-computed metal flow validated by experimental grid pattern analysis

Longitudinal sections cut through four different partially extruded billets are shown in Fig. 6 (at bottom). Before start of the extrusion experiments, the billets were fitted with an internal grid (or stripe) pattern inserted into the midplane of the billet (see left-hand side figure of top row of simulation patterns in Fig. 6). After extrusion the partially extruded billets were sectioned longitudinally to reveal the deformed internal pattern, in terms of the stripe patterns, shown (at bottom) in Fig.6. There are increasing levels of extrusion from left to right. The experimental technique used to obtain these deformed grid patterns have previously been described in detail [4].

Corresponding grid patterns recently obtained in FE-simulation of the extrusion process are shown (at top) in Fig. 6. Altogether five simulation patterns are shown; to the left the initial pattern before start of extrusion, then the four corresponding patterns as those from the experiments. How

FE-models are made, and how the deformed grid patterns are calculated by FE-models has been described in previous work [4].

As depicted by Fig.6 there is fair agreement between the grid patterns obtained in FEM-simulation and those from the experiments. The main difference between simulated and experimental flow appears in the rear-end part of the billet. Two black stripes there have been marked by letters A and B, respectively, as shown in Fig. 6. Stripe A with initially radial orientation in the billet thickens more in the core of the billet in simulation than correspondingly in the experiments. In addition, there is stripe B, with initial axial orientation in the billet. It changes its shape during extrusion as it bulges inward into the back-end region of the billet. The bulge gets more pronounced in simulation than in the experiment.

Several extrusion parameters affect metal flow in metals extrusion, and in the FE-model these parameters were set to their most realistic levels. Friction conditions on all interfaces between the billet and the tooling, for instance, was specified to be sticking friction, with exception of the interface in the die exit, i.e., in the bearing channel. Here, the friction was specified to be of Tresca-type with $m = 0.6$. Flow stress data collected in compression testing was applied for the billet material which consisted of alloy AA6082. Temperature/speed setting was; $T_b=480^\circ\text{C}$, $T_e=450^\circ\text{C}$, $T_{\text{Ram}}=50^\circ\text{C}$, $v_{\text{Ram}}=5 \text{ mms}^{-1}$.

3. Results of analysis

Our FEM-model was created using the commercial software package DEFORM 3D. When a realistic model has been established, the software allows the user to collect a lot of postprocessing information yielding information on the process conditions in the extrusion process. Some relevant results regarding the backflow of the subsurface billet layers into the rear-end of the billet during the extrusion process, and later, the outflow of this metal through the die and into the extruded rod, are presented in the subsections below.

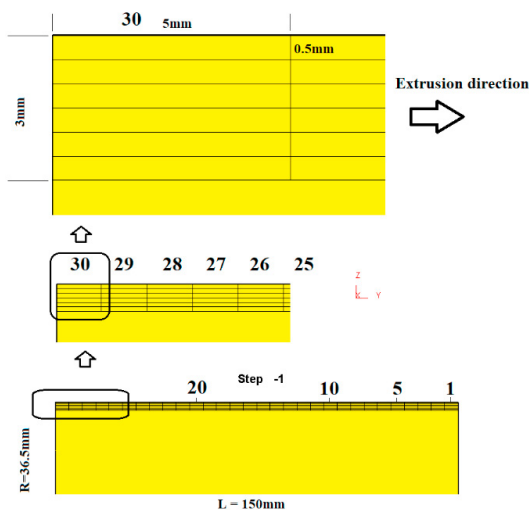


Fig. 7. Grid pattern introduced into a billet subsurface layer of 3mm thickness in simulation.

3.1. Inflow of multiple 0.5 mm thick layers of subsurface material into the billet core

In order to study how simulation describes the inflow of metal from the subsurface into the rear-end of the billet, i.e., flow type 2 (in Fig. 3), which finally leads to coring in the extruded rod, the grid pattern shown in Fig. 7 was created inside the initial billet in the simulation model.

The pattern was created in a 3 mm thick subsurface layer of the billet and consisted of rectangular grid elements of dimension 0.5mm times 5mm. The initial pattern and the deformed pattern at five different stages of extrusion are shown in Fig. 8. In order to examine the predicted distortions and the flow of the elements in the gridded subsurface layer of the billet, a radially oriented row of six rectangular elements (4th row from the rear-end of the billet) has been painted with alternating red and green color in Fig. 8.

At the top of the figure, from left to right, is first shown the initial pattern, then the pattern after the billet has been upset to fill the container. Then in the next three steps is shown how the gridded subsurface layer is scraped off from the container wall by the advancing ram as extrusion proceeds. Because of the scraping action of the ram against the container the material in the initial subsurface layer of the billet gradually accumulates as a lump of metal in the rear-end corner of the billet during the stroke. This is metal flow in terms of flow type 2. The lump grows and the subsurface layer penetrates radially inwards into the billet during the first stages of extrusion.

Fig. 8 clearly depicts that there is counter-clockwise angular rotation of the color-marked initial radially oriented row of grid elements. This is first caused by shear deformations subjected to the subsurface layers of the billet material which remain in sticking contact with the container wall.

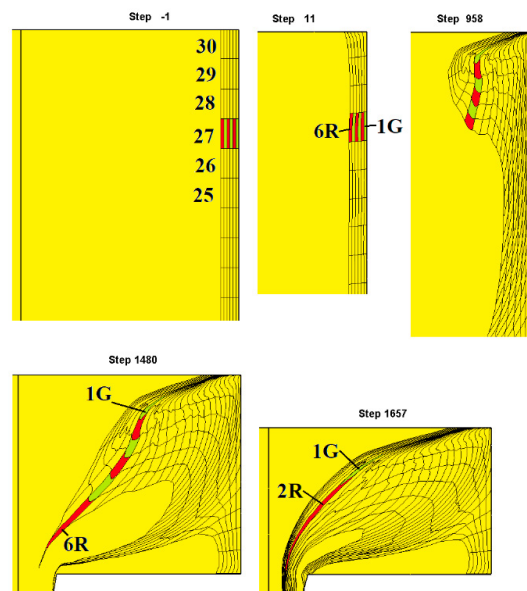


Fig. 8. FEA-predicted inflow in the rear-end of billet which causes coring.

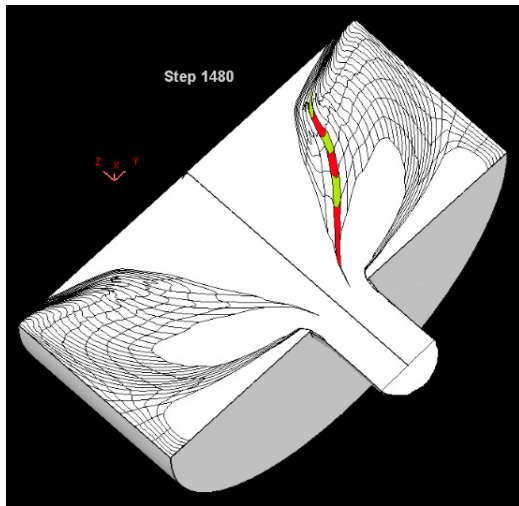


Fig. 9. Grid pattern of subsurface material approaching into the die exit.

Later, however, as the ram advances further downwards, the marked row of elements becomes scraped off from the container wall by the ram head, and now starts to flow radially inwards into the back-end of the billet. As the elements slip off from the container wall, they are subjected to additional shearing, but this time in a manner so that they change shape into approximately cube-shape. As shown in simulation step no. 958 in Fig.10, the initially radially oriented row of rectangular area elements has rotated approximately 90° counter-clockwise and now have axial orientation inside the billet.

As extrusion proceeds, the FEM-prediction is that the row of marked elements starts to flow downwards towards the die hole with gradually increasing speed, in such a manner that element 6R first approaches the die exit, then follows the other elements 5G, 4R, 3G, successively. As depicted in Fig.8, in the last shown detail in that figure, the element 2R is about to flow through the die exit. This element has now become very thin and has extended into a band-like layer. This is also the case for grid element 1G which flows right behind element 2R. It extends all the way up to the very back-end corner of the billet.

The FEA-predicted appearance of the multi-layered billet subsurface layer when it approaches into the die exit is shown in a three-dimensional view in Fig. 9.

Alternatively, the simulated material flow in the back-end corner of the billet, can be interpreted from the appearance of the grid pattern in the back-end corner region between container and ram head as depicted in Fig. 10. Here is shown how one initial radially oriented row of alternating grid elements painted white and black (top, left), located in the very back-end corner of the billet, plus additional rows (of sets) of two grid elements further down in the subsurface layer of the billet (denoted A and B), is predicted to appear later during extrusion. Moreover, in a magnified version below the same elements are shown in the same figure, at two different later stages during the extrusion stroke (Simulation step 520 and step 700).

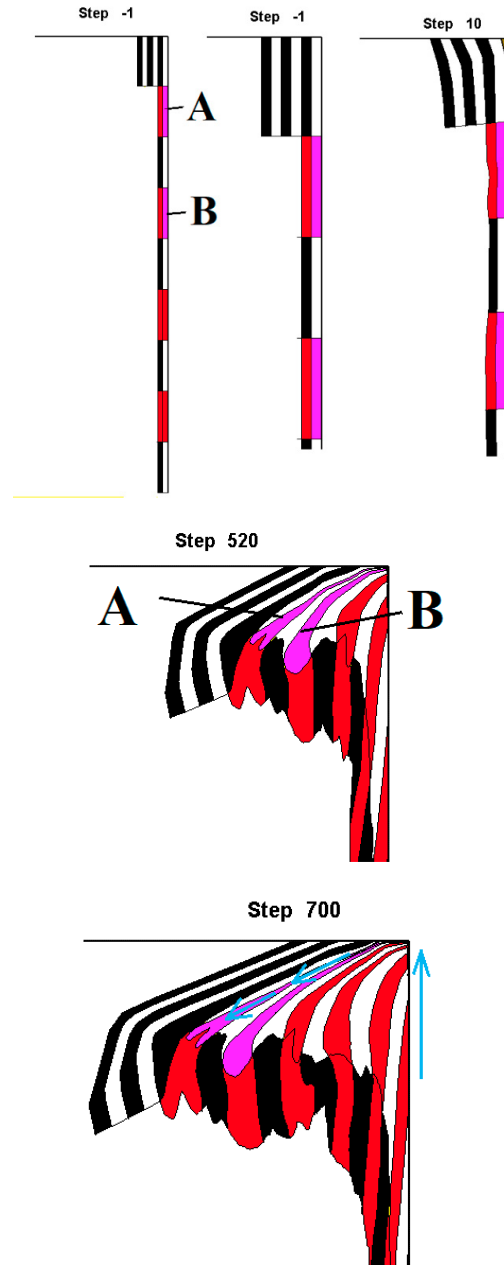


Fig. 10. Detail of simulated grid pattern from rear-end corner of billet. Arrows in billet corner shows direction of inflow of the outer subsurface billet layer into the rear-end of the billet.

As depicted in Fig. 10 the grid elements A and B are predicted to move along the path marked by blue arrows in the figure. The left-hand side of the elements, initially on the container wall, later appears connected to the tooling in the very corner between the container wall and the ram head. The other side of the elements flow in the direction of the arrows. The elements thus become stretched-out and appears as bands with curved shape extending from the back-end corner of the billet down into the interior of the billet.

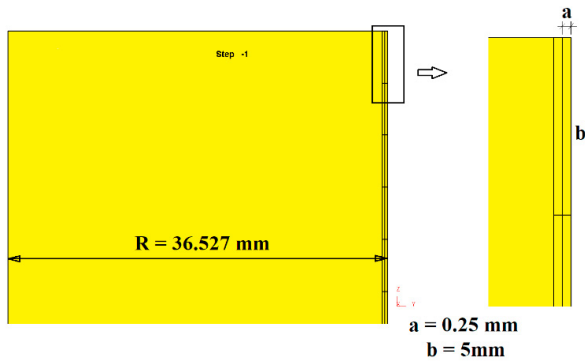


Fig. 11. Half radial section of billet with grid pattern elements of dimension $a \times b$ inserted into the subsurface of the billet, to define two outer metal layers.

3.2. Inflow of two 0.25 mm thick subsurface layers of material into the billet

The FEM-model made to reproduce the grid pattern experiment (described in sect. 2) was used to compute the inflow of two initial subsurface layers in the billet during the extrusion stroke, in a similar way as done by means of a single surface layer of contrast material in the experiments performed by Lefstad and Reiso [2]. In this computation the two layers were also partitioned into grid elements of rectangular shape, see Fig. 11.

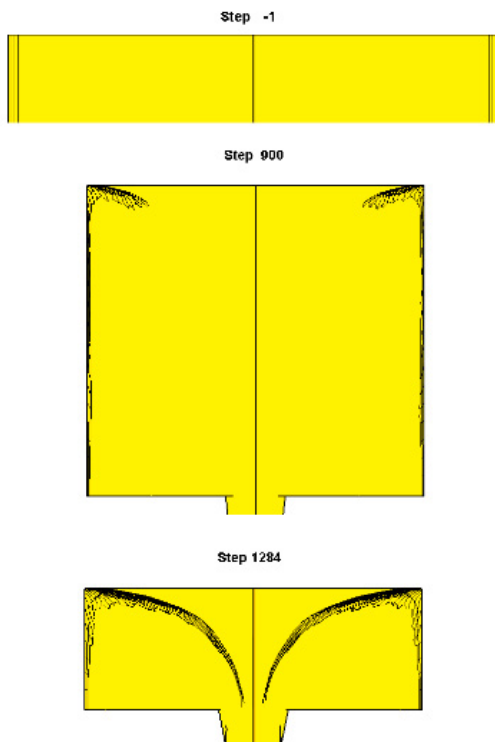


Fig. 12. Flow of two initially subsurface layers of an extruded billet causing coring as predicted by FEA.

The appearance of these two layers inside the longitudinal section of the billet at different stages during the extrusion stroke is shown in Fig. 12 and Fig. 13. The grid elements introduced into the subsurface of the billet are subjected to heavy deformations, see for instance Fig. 13(a), and become strongly distorted. The elements rotate counter clock-wise, stretch out in one direction and are thinned in the other perpendicular direction. When the metal in these layers approaches into the die exit, the grid elements have become so distorted that it is difficult to distinguish the elements from each other.

When gridded layers are replaced by layers without internal grid elements, see Fig. 13(b), it becomes easier to distinguish the individual layers in the longitudinal section of the billet.

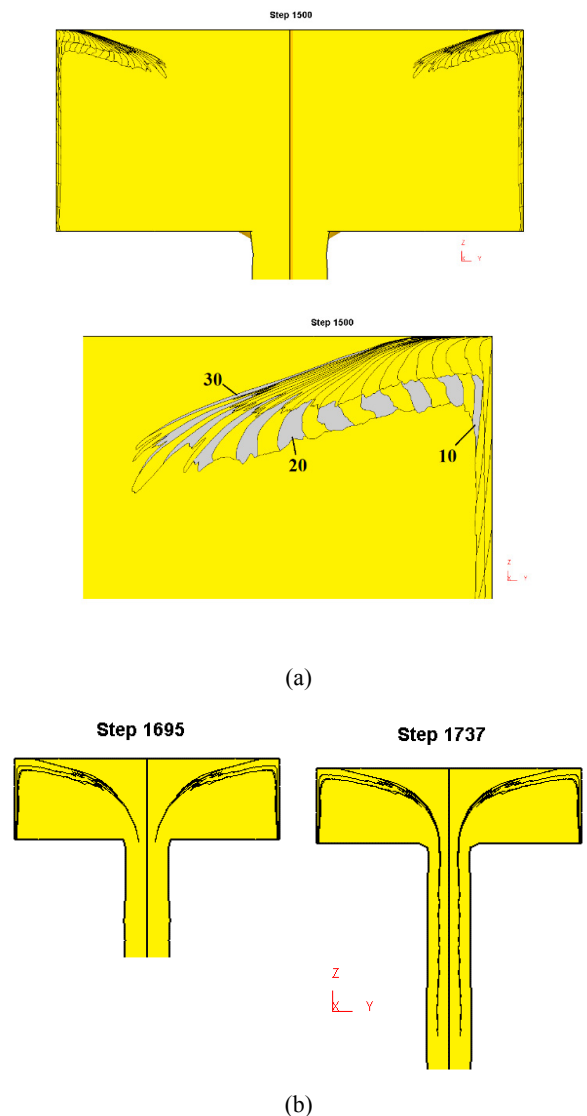


Fig. 13. Flow of two initially subsurface layers in a billet as predicted by FEA; (a)-(b) Gridded layers and (c) - (d) two layers without grid elements.

3.3. Distribution of FEA-computed state-variables inside a deforming billet

By means of the FEM-model one can compute and visualize various distributions of state variables inside any section of the billet. In Fig. 14 and Fig. 15 are shown three such distributions in the longitudinal section of the billet. At the left-hand side of Fig. 14 is shown the effective strain-rate distribution in a rather early simulation step of the extrusion process. This figure, as explained in Fig. 19.7 in [4], shows the presence of a secondary dead zone (DZ) in the rear-end of the billet with an obliquely oriented shear layer (SB) below. Below this again, there is very low strain rates in the center of the billet which shows that this region moves downwards approximately as a rigid zone (RZ).

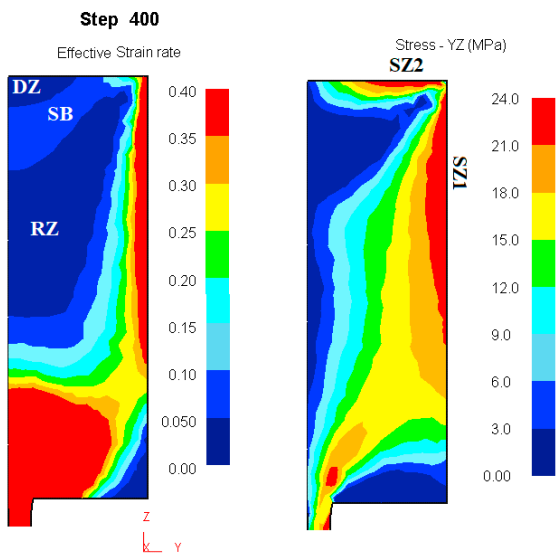


Fig. 14. Distribution of state-variables in longitudinal section of billet from FEM-model. Initial ram temperature assumed to be $T_{Ram}=50^{\circ}C$.

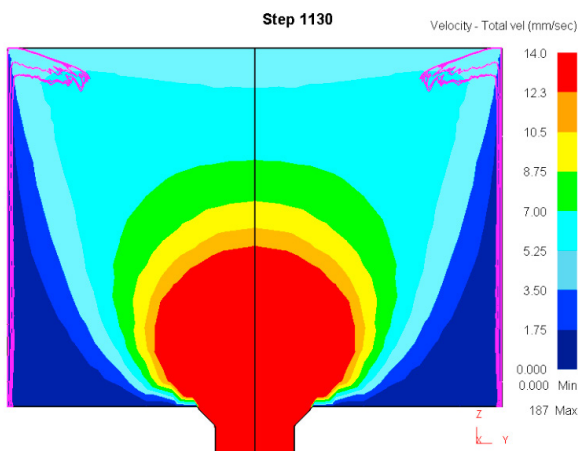


Fig. 15. Flow velocities inside billet section when the outer layers of the billet start to approach into the primary deformation zone in front of the die.

At the right-hand side of Fig. 14 is shown the distribution of the shear strain component σ_{yz} . Both distributions in Fig. 14, and particularly the distribution of the shear-strain component depicts the presence of two intense shear zones, one adjacent to the container wall (SZ1) and the other adjacent to the ram head (SZ2).

Finally, in Fig. 15 is shown a view of the longitudinal section of the billet at simulation step 1130. Here the inflow of the gridded two-layered initial subsurface layer (pink) of the billet into its back-end corner is shown, and in addition, an overlay plot of the distribution of the total velocity in the longitudinal section of the billet as computed by FEA. The figure depicts that as the flow front of the subsurface layers moves into the back-end of the billet, and downwards towards the die exit, it becomes accelerated, so that its movement speeds-up. Therefore, it penetrates faster into the core and downwards toward the die exit as it approaches closer to the die.

4. Discussion

The back-end defect coring is of great importance for the economical result in metals extrusion and has been investigated thoroughly since long ago. It affects the yield in the process, because presence of the defect is unacceptable in the final extruded profile. Common practice is therefore to leave a larger extrusion discard at the end of the stroke, than else how necessary, if this defect did not exist.

It was early understood that the coring defect forms because of radial inflow of contaminated material from the surface of the billet, or just below this surface. Because of this, a lot of information on how subsurface layers of different thicknesses flow into the interior of the billet have been collected, for instance by experiments with marker material as those presented and explained in connection with Fig. 3.

This kind of information is very useful for the extruder, as it shows to what extent inflow of contamination occurs in a given extrusion process. Despite this, there is lack of information regarding how such inflow occurs, and how the subsurface layers flowing into the rear-end of the billet behave with respect to history of deformation. As shown in the treatment in the results chapter here, such knowledge can be deduced by FEA, by introducing single or multiple subsurface layers into the billet, and, in addition, also by adding internal grid elements into each layer.

In Fig.16 are shown the initial and the partially deformed experimental grid pattern. As the figure depicts the peripheral layers of the billet (green rectangle) collects in the rear-end corner of the billet during the stroke. Because of this, the metal initially in the rear-end of the billet (blue rectangle) is compressed inwards in the radial direction and therefore must elongate axially. This is clearly visible from the figure if one looks at the two black contrast stripes in the back-end of the billet which thickens during extrusion.

The importance of having experimental evidence on how the billet deforms in metals extrusion has clearly been documented in our work.

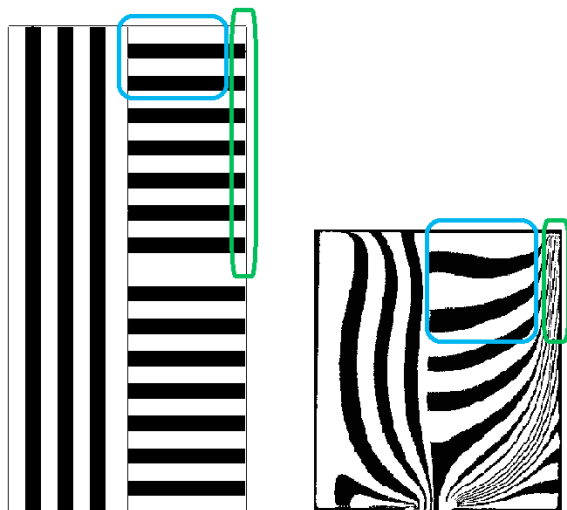


Fig. 16. Radial inflow in the back-end portion of the billet as depicted by deformed internal grid pattern.

Much efforts have been put into optimization of the FEM-model to achieve the same deformations inside the extruded billet as that shown by the grid patterns from the experiments. Finally, as depicted in Fig. 6 good resemblance was obtained between the FEA-computed grid pattern, and the corresponding experimental pattern. However, there are still some deviation between the two. While there is very close agreement between simulation and experiment in the first 1/3rd of the extrusion process, there is increasing degree of disagreement throughout the rest of the extrusion process. The disagreement manifests itself in that there is predicted somewhat faster outflow of the material in the center of the billet in FEA than in experiment.

By means of use of different purpose-made internal grid-patterns introduced into the subsurface layers of the initial billet, a detailed description is given here, of the nature of the inwards metal flow experienced in the extrusion process. This is discussed in connection with Fig. 7-13 presented here.

The study performed reveals that inflow leading to the coring defect in extrusion occurs by a mechanism where the subsurface layers of the billet first deforms in shear against the container wall. This occurs because the billet surface sticks to the container wall in extrusion. However, as the ram head advances forward down into the container, its edge will catch up with the sheared material on the container wall, so that the material becomes scraped off from the wall by the advancing ram edge, and this material therefore starts to flow radially inwards into the rear-end of the billet. Additional shear deformations are subjected to the subsurface material, as it, in

this way, shifts its direction of movement in the back-end corner of the billet.

After this, the material from the sub-surface of the billet slides slowly inwards along the ram surface, where the secondary dead zone (DZ2) of stagnant billet material is present. Because of this, the subsurface material now gradually shifts its inwards radial direction of movement, to become more and more directed in the direction of the ram movement down towards the die exit. The subsurface layers material thus flow against the stagnant metal zone present in the rear-end of the billet. As the subsurface layer moves further down into the billet, the material becomes accelerated forward with gradually increasing speed downwards towards the die exit. This flow of the subsurface layer of material as predicted in simulation, is perhaps best illustrated by the picture shown in Fig. 9.

5. Conclusions

A 3-dimensional DEFORM FEM-model of an axis-symmetric laboratory process have been established. The model is an approximately 2-factor scaled-down version of common industrial extrusion. Calculations performed with internal grid patterns inside the billet documents good similarity in metal flow in simulation and previously performed extrusion experiments.

By introduction of purpose-made grid patterns into single or multiple subsurface layers of the billet it is possible to make detailed studies on how the surface material moves down into the region in the back-end of the billet during extrusion. In the late stages of the extrusion process, this material flows further through the die hole and out in the extrusion, where it causes formation of the internal defect commonly named coring.

The FEM-model clearly describes in which sequence different parts of the billet subsurface layer moves downwards into the back-end of the billet, and how it penetrates further down through the die and into the extrudate. Furthermore, the model describes the deformation behavior and history of deformation of this material during the extrusion process.

References

- [1] Valberg H. The surface formation in metals extrusion. Ph.D-thesis, NTNU, 1987.
- [2] Lefstad M, Reiso O, and Johnsen V. Flow of the billet surface in aluminium extrusion. Proc. Int. Al Extr. Techn. Sem. 1993;2:503.
- [3] Hatzenbichler T, Buchmayr B. Finite element method simulation of internal defects in billet-to-billet extrusion. Proc. of the Inst. of Mech. Eng., Part B: J. of Eng. Manufact., 2010, 224.7: 1029-1042.
- [4] Valberg H. Applied metal forming; Including FEM analysis. Cambridge University Press 2010.